

An iterative representation for electrically-conducting Maxwell fluid bounded by a wedge-shaped wall

Emran Khoshrouye Ghiasi¹, Wuriti Sridhar^{2,*}

¹ *Young Researchers and Elite Club, Mashhad Branch, Islamic Azad University, Mashhad, Iran*

² *Department of Mathematics, Koneru Lakshmaiah Education Foundation, Vaddeswaram, Guntur-522502, India*

Abstract

This paper is devoted to obtaining convergent series expansion for the flow of electrically-conducting Maxwell fluid past a wedge-shaped wall proposed in a recent study by Abbasbandy et al. [Abbasbandy, S., Naz, R., Hayat, T., Alsaedi, A.: Numerical and analytical solutions for Falkner-Skan flow of MHD Maxwell fluid. Appl. Math. Comput. 242, 569-575 (2014)]. It is found that the 9th-order homotopy approach converges sufficiently rapidly for the case $\hbar = -0.442$. Furthermore, the reliability of the present solution through some direct comparisons was verified.

Keywords: Maxwell fluid, Local velocity distribution, Convergence, Auxiliary parameter, P-time

1. Introduction

The Maxwell fluid is a viscoelastic non-Newtonian material, where the mathematical characters of governing equations vary only with a small degree of compressibility [1]. A major success of these materials is that they have been investigated by so many researchers in the last two decades [2-16]. It is noteworthy that one of the most powerful methodologies for finding the velocity, temperature and nanoparticle concentration (if any) distributions is the homotopy approach which is genuinely effective, and does not depend on any small or large physical properties [17-27]. In 2012, Hayat et al. [28] presented a unique solution for the mixed convection Maxwell fluid past a wedge-shaped wall. They could show that their approach does not suffer from long processing time (P-time), and is uniformly valid throughout the domain of convergence. Furthermore, Abbasbandy et al. [29], Asaithambi [30] and Abbasbandy and Mustafa [31] developed other solutions for the same geometry that included Chebyshev collocation method (CCM), Runge-Kutta method (RKM) and homotopy-Padé technique, respectively.

It is to be mentioned here that, this paper investigates the additional convergence of electrically-conducting Maxwell fluid over a wedge-shaped wall. To the best of the author's knowledge, there is no work dealing with this issue yet.

2. Theoretical formulation

Consider an electrically-conducting fluid flow bounded by a wedge-shaped wall, where the pressure gradient is approximately zero. According to basic hypothesis of the Maxwell fluid type, the continuity and boundary-layer x -momentum equations can be expressed as [32],

$$u_{,x} + v_{,y} = 0, \quad (1a)$$

$$uu_{,x} + vv_{,y} + \alpha(u^2u_{,xx} + v^2v_{,yy} + 2uvu_{,xy}) = UU_{,x} + vv_{,yy} - \frac{\sigma B^2 \sin^2 \theta}{\rho} (u - U + \alpha u_{,y}), \quad (1b)$$

with the boundary conditions,

$$\begin{aligned} u = 0, v = 0, \quad \text{at } y = 0, \\ u = U(x) = \lambda x, \quad \text{as } y \rightarrow \infty, \end{aligned} \tag{2}$$

where u and v are the velocity components along and perpendicular to the x - and y -directions, respectively, α is the relaxation time, U is the characteristic velocity, ν is the kinematic viscosity, σ is the electrical conductivity, B is the magnetic field strength, θ is the inclination angle of the magnetic field, ρ is the density and λ is the stretching rate.

Upon introducing the variables $\eta = \sqrt{\frac{\lambda}{\nu}}y$, $u = \lambda x \varphi_{,\eta}$ and $v = -\sqrt{\lambda \nu} \varphi$, the governing equation and associated boundary conditions are attained by,

$$\varphi_{,\eta\eta\eta} + (1 + \gamma H^2) \varphi \varphi_{,\eta\eta} + (1 - \varphi_{,\eta}^2) + H^2 \sin^2 \theta (1 - \varphi_{,\eta}) + 2\gamma \varphi \varphi_{,\eta} \varphi_{,\eta\eta} - \gamma \varphi^2 \varphi_{,\eta\eta\eta} = 0, \tag{3}$$

$$\begin{aligned} \varphi = 0, \varphi_{,\eta} = 0, \quad \text{at } \eta = 0, \\ \varphi_{,\eta} = 1, \quad \text{as } \eta \rightarrow \infty, \end{aligned} \tag{4}$$

where $\gamma = \alpha \lambda$ and $H = \sqrt{\frac{\sigma B^2}{\lambda \rho}}$ are the Maxwell fluid parameter and Hartmann number, respectively.

Here, the dimensionless quantity skin friction coefficient takes the form [33],

$$\sqrt{Re_x} C_f = (1 + \gamma) \varphi_{,\eta\eta}(0), \tag{5}$$

where $Re_x = \frac{xU}{\nu}$ is the local Reynolds number.

3. Solution methodology

Let us define the general nonlinear problem in the following form,

$$\mathcal{N}[\varphi(\eta)] =, \tag{6}$$

where \mathcal{N} is a nonlinear operator. Using $p \in [0,1]$ as an embedding parameter, the homotopy function is assumed to be [34],

$$\mathcal{H}(\bar{\varphi}; p, \hbar) = (1 - p) \mathcal{L}[\bar{\varphi}(\eta; p) - \varphi_0(\eta)] + p \hbar \mathcal{N}[\bar{\varphi}(\eta; p)], \tag{7}$$

where $\bar{\varphi}$ is an unknown function of η and p , $\hbar \neq 0$ is an auxiliary parameter, \mathcal{L} is an auxiliary linear operator and φ_0 is an initial guess of φ . It is to be noted here that, in the limit as p approaches 0 and 1, $\bar{\varphi}(\eta; p)$ varies from the initial guess to the solution of $\varphi(\eta)$. Therefore, $\bar{\varphi}(\eta; 0) = \varphi_0(\eta)$ and

$\bar{\varphi}(\eta; 1) = \varphi(\eta)$ can be considered as the solution of $\mathcal{H}(\bar{\varphi}; p, \hbar)|_{p=0} = 0$ and $\mathcal{H}(\bar{\varphi}; p, \hbar)|_{p=1} = 0$, respectively.

By expanding $\bar{\varphi}(\eta; p)$ in a Taylor's series with respect to p , one would obtain,

$$\bar{\varphi}(\eta; p) = \bar{\varphi}(\eta; 0) + \sum_{j=1}^{\infty} \frac{1}{j!} \bar{\varphi}_{,p}^{(j)}(\eta; p)|_{p=0} = \varphi_0(\eta) + \sum_{j=1}^{\infty} \varphi_j(\eta) p^j, \quad (8)$$

where φ_j is the j th-order deformation derivative.

By equating the homotopy function given in Eq. (7) to zero and setting $p = 0$, the zeroth-order deformation equation is constructed as [34],

$$\mathcal{L}[\bar{\varphi}(\eta; 0) - \varphi_0(\eta)] = 0. \quad (9)$$

Also, differentiating $\mathcal{H}(\bar{\varphi}; p, \hbar) = 0$ j times with respect to p , setting $p = 0$ and dividing it by $j!$, *after dropping the hats*, gives the following j th-order deformation equation,

$$\mathcal{L}[\varphi_j(\eta) - \chi_j \varphi_{j-1}(\eta)] + \frac{1}{(j-1)!} \hbar \mathcal{N}_{,p}^{(j-1)}[\varphi(\eta; p)]|_{p=0} = 0, \quad (10)$$

where,

$$\chi_j = \begin{cases} 0, & j \leq 1, \\ 1, & j > 1. \end{cases} \quad (11)$$

Here, the initial guess and auxiliary linear operator are appropriately as,

$$\varphi_0(\eta) = \eta - (1 - e^{-\eta}), \quad (12)$$

$$\mathcal{L}[\varphi(\eta; p)] = \varphi_{,\eta\eta\eta}(\eta; p) - \varphi_{,\eta}(\eta; p), \quad (13)$$

with the property,

$$\mathcal{L}[\beta_1 + \beta_2 e^{\eta} + \beta_3 e^{-\eta}] = 0, \quad (14)$$

where β_1 - β_3 are the integration constants.

The Taylor's series expansion for $\varphi(\eta; p)$ can be seen by rewriting Eq. (8) in the form,

$$\varphi(\eta; p) = \varphi_0(\eta) + p\varphi_1(\eta) + p^2\varphi_2(\eta) + \dots \quad (15)$$

The nonlinear operator in this case becomes,

$$\begin{aligned} \mathcal{N}[\varphi(\eta; p)] = & \varphi_{,\eta\eta\eta}(\eta; p) + (1 + \gamma H^2)\varphi(\eta; p)\varphi_{,\eta\eta}(\eta; p) + \left(1 - \varphi_{,\eta}^2(\eta; p)\right) \\ & + H^2 \sin^2 \theta \left(1 - \varphi_{,\eta}(\eta; p)\right) + 2\gamma\varphi(\eta; p)\varphi_{,\eta}(\eta; p)\varphi_{,\eta\eta}(\eta; p) - \gamma\varphi^2\varphi_{,\eta\eta\eta}(\eta; p), \end{aligned} \quad (16)$$

with the boundary conditions,

$$\begin{aligned} \varphi(\eta; p) = 0, \varphi_{,\eta}(\eta; p) = 0, & \quad \text{at } \eta = 0, \\ \varphi_{,\eta}(\eta; p) = 1, & \quad \text{as } \eta \rightarrow \infty. \end{aligned} \tag{17}$$

The zeroth-order deformation equation is constructed as,

$$\varphi_{,\eta\eta\eta}(\eta) - \varphi_{0,\eta}(\eta) = 0, \tag{18}$$

which goes to zero boundary conditions.

The j th-order deformation equation is given by,

$$\varphi_{j,\eta\eta\eta}(\eta) - \varphi_{j,\eta}(\eta) = \chi_j \left(\varphi_{j-1,\eta\eta\eta}(\eta) - \varphi_{j-1,\eta}(\eta) \right) - \frac{1}{(j-1)!} \hbar \mathcal{N}_{,p}^{(j-1)}[\varphi(\eta; p)]|_{p=0} = 0. \tag{19}$$

After finding the integration constants β_1 - β_3 , by setting $p = 1$, the j th-order approximate solution is generated as,

$$\varphi_j(\eta) = \varphi_j^\blacksquare(\eta) - \varphi_j^\blacksquare(0)(1 - e^{-\eta}) - \varphi_{j,\eta}^\blacksquare(0), \tag{20}$$

where $\varphi_j^\blacksquare(\eta)$ is a particular solution. Therefore, the k th-order approximate solution yields,

$$\varphi_k(\eta) = \sum_{j=0}^k \varphi_j(\eta). \tag{21}$$

4. Results and discussion

To validate the accuracy and efficiency of the present solution, the geometric and physical properties, unless outlined otherwise, are provided as $\gamma = 0.3$, $H = 1$ and $\theta = 45^\circ$. It is to be mentioned here that, these parameters are matched with the case investigated by Abbasbandy et al. [32], which consisted of bounds on the convergence, not calculations for the actual rate of convergence. In addition, due to Abbasbandy et al. [32], the auxiliary parameter in this case is taken as $\hbar = -0.45$. In Table 1, the present solution is compared with those reported by Abbasbandy et al. [29], Asaithambi [30] and Abbasbandy and Mustafa [31].

According to the results given in Table 1, by increasing the values of Maxwell fluid parameter, the skin friction coefficient in all cases is enhanced; because for large γ the fluid behaves as a very stiff elastic material. In addition, the 9th-order homotopy approach agrees well with those of Abbasbandy et al. [29], Asaithambi [30] and Abbasbandy and Mustafa [31] with an incurred error of at most 2.11%, 1.88% and 0.03%, respectively. Therefore, it can be concluded that the 9th-order homotopy approach provides more accurate results than those of 5th- and 7th-order ones. However, the discrepancies between the present solution and those of CCM and RKM findings could be due to the algebraic nature of numerical manipulation.

It is worth noting that a further reduction of P-time can be obtained by considering the square residual error as [35],

$$\Delta_k = \frac{1}{n+1} \sum_{m=0}^n \left(\mathcal{N} \left[\sum_{l=0}^k \varphi_l(\eta) \right]_{\eta=md\eta} \right)^2. \tag{22}$$

It is to be noted here that solving $\Delta_{k,\hbar} = 0$ in terms of \hbar and using the fact that $-0.5 \leq \hbar \leq -0.39$ [1], is necessary and sufficient to minimize the square residual error of any order.

To find the admissible value of auxiliary parameter, one should draw the variation of square residual error versus different values of \hbar . Then, for any minimum choice of resulting configuration, the admissible value of auxiliary parameter will be found explicitly. This issue is shown in Fig. 1 for $k = 9$.

As it is seen from Fig. 1, the square residual error achieves its minimum possible values when the auxiliary parameter is selected as $\hbar = -0.442$. Furthermore, as one would expect, the P-time is then reduced through the use of Eq. (22).

Table 2 investigates convergence and uniqueness of the series expansion for the values of auxiliary parameter, square residual error and P-time with $k = 5, 7$ and 9 . It can be observed from this table that the square residual error approaches zero as k tends to infinity. Therefore, in view of the results provided in Tables 1 and 2 and Fig. 1, one can say that *employing the homotopy approach is essential to accelerate rate of convergence without any loss of accuracy*.

A comparison of the local velocity distribution using the admissible value of auxiliary parameter obtained through the homotopy approach is depicted in Fig. 2. This figure also represents verifications for the converged local velocity distribution compared with those of Abbasbandy et al. [29]. According to

Fig. 2, it is observed that the 9th-order homotopy approach for the case of $\hbar = -0.442$ agrees remarkably well with the numerical findings reported by Abbasbandy et al. [29]. That is due to the fact that the homotopy approach is essentially divergence free when the square residual error given in Eq. (22) is employed. Accordingly, it is to be mentioned here that $\hbar = -0.442$ can give accurate answers to the question of how an electrically-conducting Maxwell fluid flow past a wedge-shaped wall behaves. Here, for the sake of brevity, only the converged local velocity distribution versus some different γ is presented in Table 3.

Based on the results listed in Table 3, the converged local velocity distribution satisfies Eq. (4) at $\eta = 3$. It is to be noted that the abovementioned criterion is most useful for finding exact solutions of highly nonlinear problems especially large in the case of series expansion.

5. Conclusions

This paper was aimed to investigate briefly the flow of Maxwell fluid past a wedge-shaped wall, and also provide a convergence criterion for the comparison studies. It was shown that the 9th-order homotopy approach could give high-accuracy approximations than those of 5th- and 7th-order ones for the local velocity distribution and skin friction coefficient.

Acknowledgement

The authors would like to thank the editor and reviewers for their helpful comments.

Nomenclatures

B	Magnetic field strength	$\text{kg s}^{-2} \text{A}^{-1}$
C_f	Skin friction coefficient	-
H	Hartmann number	-
Re_x	Local Reynolds number	-
U	Characteristic velocity	m s^{-1}
u, v	Velocity components along and perpendicular to the x - and y -directions, respectively	m s^{-1}

Greek symbols

α	Relaxation time	s
γ	Maxwell fluid parameter	-
η	Similarity variable	-
θ	Inclination angle of the magnetic field	-
λ	Stretching rate	s^{-1}
ν	Kinematic viscosity	$m^2 s^{-1}$
ρ	Density	$kg m^{-3}$
σ	Electrical conductivity	$S m^{-1}$
φ	Similarity function	-

References

1. Sequeira, A., da Veiga, H.B., Videman, J.H.: Applied Nonlinear Analysis. Springer, New York (2002)
2. Hayat, T., Sajjad, R., Abbas, Z., Sajid, M., Hendi, A.A.: Radiation effects on MHD flow of Maxwell fluid in a channel with porous medium. *Int. J. Heat Mass Transfer* **54**(4), 854-862 (2011). <https://doi.org/10.1016/j.ijheatmasstransfer.2010.09.069>
3. Imran, M.A., Riaz, M.B., Shah, N.A., Zafar, A.A.: Boundary layer flow of MHD generalized Maxwell fluid over an exponentially accelerated infinite vertical surface with slip and Newtonian heating at the boundary. *Results Phys.* **8**, 1061-1067 (2018). <https://doi.org/10.1016/j.rinp.2018.01.036>
4. Kumar, M.S., Sandeep, N., Kumar, B.R., Saleem, S.: A comparative study of chemically reacting 2D flow of Casson and Maxwell fluids. *Alexandria Eng. J.* **57**(3), 2027-2034 (2018). <https://doi.org/10.1016/j.aej.2017.05.010>
5. Ramesh, G.K., Gireesha, B.J., Hayat, T., Alsaedi, A.: Stagnation point flow of Maxwell fluid towards a permeable surface in the presence of nanoparticle. *Alexandria Eng. J.* **55**(2), 857-865 (2016). <https://doi.org/10.1016/j.aej.2016.02.007>
6. Aman, S., Al-Mdallal, Q., Khan, I.: Heat transfer and second order slip effect on MHD flow of fractional Maxwell fluid in a porous medium. *J. King Saud Univ.* (2018). <https://doi.org/10.1016/j.jksus.2018.07.007> (**In Press**)
7. Mukhopadhyay, S., De, P.R., Layek, G.C.: Heat transfer characteristics for the Maxwell fluid flow past an unsteady stretching permeable surface embedded in a porous medium with thermal radiation. *J. Appl. Mech. Tech. Phys.* **54**(3), 385-396 (2013). <https://doi.org/10.1134/S0021894413030061>
8. Shah, S., Hussain, S., Sagheer, M.: Thermal stratification effects on mixed convective Maxwell fluid flow with variable thermal conductivity and homogeneous/heterogeneous reactions. *J. Braz. Soc. Mech. Sci. Eng.* **40**(9), 1-15 (2018). <https://doi.org/10.1007/s40430-018-1363-6>
9. Kumari, M., Nath, G.: Steady mixed convection flow of Maxwell fluid over an exponentially stretching vertical surface with magnetic field and viscous dissipation. *Meccanica* **49**(5), 1263-1274 (2014). <https://doi.org/10.1007/s11012-014-9884-2>
10. Murtaza, M.G., Ferdows, M.: Three-dimensional biomagnetic Maxwell fluid flow over a stretching surface in presence of heat source/sink. *Int. J. Biomath.* **12**(3), 1-19 (2019). <https://doi.org/10.1142/S1793524519500360>
11. Shehzad, S.A., Qasim, M., Alsaedi, A., Hayat, T., Alsaadi, F.: Radiative Maxwell fluid flow with variable thermal conductivity due to a stretching surface in a porous medium. *J. Aerospace Eng.* **27**(5), 1-7 (2014). [https://doi.org/10.1061/\(ASCE\)AS.1943-5525.0000332](https://doi.org/10.1061/(ASCE)AS.1943-5525.0000332)

12. Arifuzzaman, S.M., Khan, M.S., Islam, M.S., Islam, M.M., Rana, B.M., Biswas, P., Ahmmed, S.F.: MHD Maxwell fluid flow in presence of nano-particle through a vertical porous-plate with heat-generation, radiation absorption and chemical reaction. *Front. Heat Mass Transfer* **9**, 1-15 (2017). <https://doi.org/10.5098/hmt.9.25>
13. Omowaye, A.J., Animasaun, I.L.: Upper-convected Maxwell fluid flow with variable thermo-physical properties over a melting surface situated in hot environment subject to thermal stratification. *J. Appl. Fluid Mech.* **9**(4), 1777-1790 (2016). <https://doi.org/10.18869/acadpub.jafm.68.235.24939>
14. Hayat, T., Hina, S., Watif, A., Hendi, A.: Slip effects on peristaltic transport of a Maxwell fluid with heat and mass transfer. *J. Mech. Med. Biol.* **12**(1), 1-22 (2012). <https://doi.org/10.1142/S0219519412004375>
15. Hayat, T., Ali, N., Asghar, S.: Hall effects on peristaltic flow of a Maxwell fluid in a porous medium. *Phys. Lett. A* **363**(5-6), 397-403 (2007). <https://doi.org/10.1016/j.physleta.2006.10.104>
16. Kashyap, K.P., Ojjela, O., Das, S.K.: Magnetohydrodynamic mixed convective flow of an upper convected Maxwell fluid through variably permeable dilating channel with Soret effect. *Pramana* **92**(5), 1-10 (2019). <https://doi.org/10.1007/s12043-019-1732-4>
17. Khoshrouye Ghiasi, E., Saleh, R.: Constructing analytic solutions on the Tricomi equation. *Open Phys.* **16**(1), 143-148 (2018). <https://doi.org/10.1515/phys-2018-0022>
18. Khoshrouye Ghiasi, E., Saleh, R.: Unsteady shrinking embedded horizontal sheet subjected to inclined Lorentz force and Joule heating, an analytical solution. *Results Phys.* **11**, 65-71 (2018). <https://doi.org/10.1016/j.rinp.2018.07.026>
19. [19] Khoshrouye Ghiasi, E., Saleh, R.: Optimal homotopy asymptotic method-based Galerkin approach for solving generalized Blasius boundary value problem. *J. Adv. Phys.* **7**(3), 408-411 (2018). <https://doi.org/10.1166/jap.2018.1435>
20. Khoshrouye Ghiasi, E., Saleh, R.: A convergence criterion for tangent hyperbolic fluid along a stretching wall subjected to inclined electromagnetic field. *SeMA J.* **76**(3), 521-531 (2019). <https://doi.org/10.1007/s40324-019-00190-1>
21. Khoshrouye Ghiasi, E., Saleh, R.: 2D flow of Casson fluid with non-uniform heat source/sink and Joule heating. *Front. Heat Mass Transfer* **12**, 1-7 (2019). <https://doi.org/10.5098/hmt.12.4>
22. Khoshrouye Ghiasi, E., Saleh, R.: HBA analysis of generalized viscoelastic fluids. *Eng. Appl. Sci. Lett.* **2**(3), 7-13 (2019). <https://doi.org/10.30538/psrp-easl2019.0022>
23. Khoshrouye Ghiasi, E., Saleh, R.: Nonlinear stability and thermomechanical analysis of hydromagnetic Falkner-Skan Casson conjugate fluid flow over an angular-geometric surface based on Buongiorno's model using homotopy analysis method and its extension. *Pramana* **92**(1), 1-12 (2019). <https://doi.org/10.1007/s12043-018-1667-1>
24. Khoshrouye Ghiasi, E., Saleh, R.: Analytical and numerical solutions to the 2D Sakiadis flow of Casson fluid with cross diffusion, inclined magnetic force, viscous dissipation and thermal radiation based on Buongiorno's mathematical model. *CFD Lett.* **11**(1) 40-54, (2019)
25. Khoshrouye Ghiasi, E., Saleh, R.: On approximation of FBVP by homotopy-based truncation technique. *SeMA J.* **76**(4), 553-558 (2019). <https://doi.org/10.1007/s40324-019-00193-y>
26. Khoshrouye Ghiasi, E., Saleh, R.: Non-dimensional optimization of magnetohydrodynamic Falkner-Skan fluid flow. *INAE Lett.* **3**(3), 143-147 (2018). <https://doi.org/10.1007/s41403-018-0043-2>
27. Khoshrouye Ghiasi, E., Saleh, R.: Homotopy analysis method for Sakiadis flow of thixotropic fluid. *Eur. Phys. J. Plus* **134**(1), 1-9 (2019). <https://doi.org/10.1140/epjp/i2019-12449-9>
28. Hayat, T., Farooq, M., Iqbal, Z., Alsaedi, A.: Mixed convection Falkner-Skan flow of a Maxwell fluid. *J. Heat Transfer* **134**(11), 1-6 (2012). <https://doi.org/10.1115/1.4006897>

29. Abbasbandy, S., Hayat, T., Ghehsareh, H.R., Alsaedi, A.: MHD Falkner-Skan flow of Maxwell fluid by rational Chebyshev collocation method. *Appl. Math. Mech. –Eng. Ed.* **34**(8), 921-930 (2013). <https://doi.org/10.1007/s10483-013-1717-7>
30. Asaithambi, N.S.: A numerical method for the solution of the Falkner-Skan equation. *Appl. Math. Comput.* **81**(2-3), 259-264 (1997). [https://doi.org/10.1016/s0096-3003\(95\)00325-8](https://doi.org/10.1016/s0096-3003(95)00325-8)
31. Abbasbandy, S., Mustafa, M.: Analytical and numerical approaches for Falkner-Skan flow of MHD Maxwell fluid using a non-Fourier heat flux model. *Int. J. Numer. Methods Heat Fluid Flow* **28**(7), 1539-1555 (2018). <https://doi.org/10.1108/HFF-08-2017-0316>
32. Abbasbandy, S., Naz, R., Hayat, T., Alsaedi, A.: Numerical and analytical solutions for Falkner-Skan flow of MHD Maxwell fluid. *Appl. Math. Comput.* **242**, 569-575 (2014). <https://doi.org/10.1016/j.amc.2014.04.102>
33. Ramesh, G.K., Gireesha, B.J., Hayat, T., Alsaedi, A.: Stagnation point flow of Maxwell fluid towards a permeable surface in the presence of nanoparticles. *Alexandria Eng. J.* **55**(2), 857-865 (2016). <https://doi.org/10.1016/j.aej.2016.02.007>
34. Liao, S.J.: *Beyond perturbation: Introduction to the homotopy analysis method.* Chapman & Hall/CRC Press, Boca Raton (2003)
35. Liao, S.J.: An optimal homotopy-analysis approach for strongly nonlinear differential equations. *Commun. Nonlinear Sci. Numer. Simulat.* **15**(8), 2003-2016 (2010). <https://doi.org/10.1016/j.cnsns.2009.09.002>

Figure captions

Fig. 1 Selection of admissible value of auxiliary parameter

Fig. 2 Influence of the auxiliary parameter on the local velocity distribution with the property $\gamma = 0.5$

Table 1 Verification of the skin friction coefficient obtained by different solution methodologies

γ	Present ($\hbar = -0.45$)			Abbasbandy et al. [29]	Asaithambi [30]	Abbasbandy and Mustafa [31]
	$k = 5$	$k = 7$	$k = 9$			
0	1.58531544	1.58532210	1.58532792	1.58534427	1.585339	1.58533068
0.25	1.63420170	1.63420659	1.63421109	1.63413446	1.634145	1.63421469
0.5	1.68508842	1.68509517	1.68509991	1.68535001	1.685494	1.68510977
0.75	1.73643499	1.73644106	1.73644615	1.73698860	1.736842	1.73645170
1	1.78752090	1.78752755	1.78753296	1.78849101	1.788302	1.78753609

Table 2 Convergence of the series expansion, when the value of P-time is rounded up to two digits

η	$k = 5$			$k = 7$			$k = 9$		
	\hbar_{adm}	Δ_k	P-time (s)	\hbar_{adm}	Δ_k	P-time (s)	\hbar_{adm}	Δ_k	P-time (s)
0	-0.427	4.39×10^{-8}	7.02	-0.436	9.54×10^{-9}	15.34	-0.442	7.03×10^{-9}	38.20
0.2	-0.427	5.14×10^{-8}	7.02	-0.436	1.03×10^{-8}	15.34	-0.442	8.76×10^{-9}	38.20
0.4	-0.427	6.10×10^{-8}	7.02	-0.436	2.59×10^{-8}	15.34	-0.442	9.80×10^{-9}	38.20
0.6	-0.427	6.98×10^{-8}	7.02	-0.436	3.72×10^{-8}	15.34	-0.442	1.08×10^{-8}	38.20
0.8	-0.427	7.71×10^{-8}	7.02	-0.436	4.50×10^{-8}	15.34	-0.442	2.39×10^{-8}	38.20
1	-0.427	8.64×10^{-8}	7.02	-0.436	5.25×10^{-8}	15.34	-0.442	3.84×10^{-8}	38.20

Table 3 Variation of the local velocity distribution versus γ

η	$\varphi_{,\eta} (\gamma = 0)$	$\varphi_{,\eta} (\gamma = 1)$	$\varphi_{,\eta} (\gamma = 2)$	$\varphi_{,\eta} (\gamma = 3)$
0	0	0	0	0
0.5	0.2417	0.3809	0.4278	0.4326
1	0.5396	0.6663	0.7099	0.7217
1.5	0.6911	0.8814	0.9015	0.9416
2	0.8071	0.9560	0.9810	1
2.5	0.9255	1	1	1
3	1	1	1	1

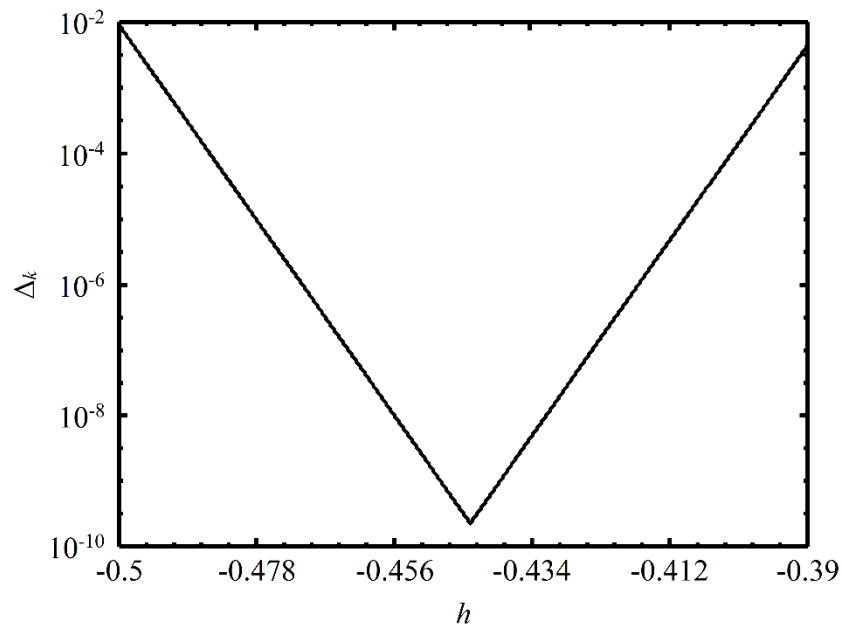


Fig. 1 Selection of admissible value of auxiliary parameter

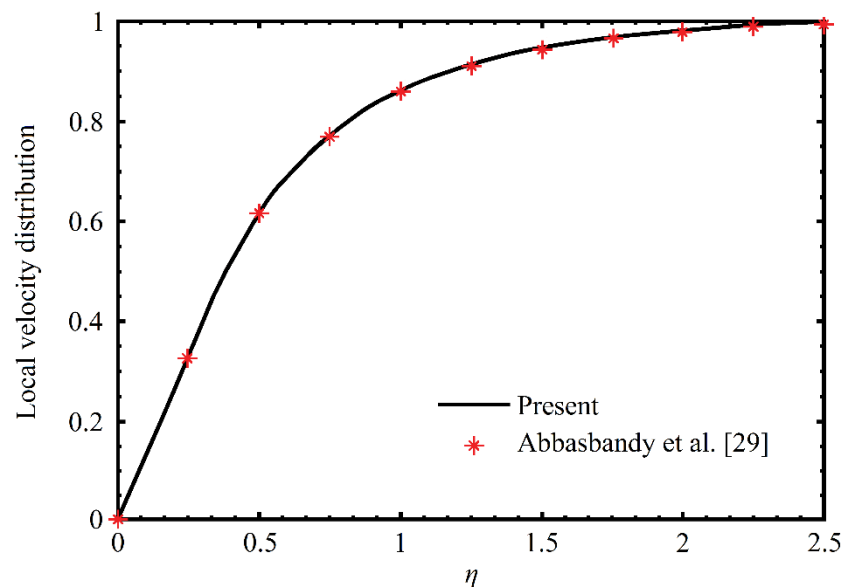


Fig. 2 Influence of the auxiliary parameter on the local velocity distribution with the property $\gamma = 0.5$